UC Davis
UC Davis Previously Published Works

Title

Chemical and structural characterization of EUV photoresists as a function of depth by standing-wave x-ray photoelectron spectroscopy

Permalink

Journal

ISSN

Authors

Conti, Giuseppina
Martins, Henrique P
Cordova, Isvar A
et al.

Publication Date

DOI

Chemical and structural characterization of EUV photoresists as a function of depth by standing-wave x-ray photoelectron spectroscopy

Giuseppina Conti⊙,[a,b,*] Henrique P. Martins⊙,[a,b] Isvar A. Cordova,[c]
Jonathan Ma⊙,[c] Rudy J. Wojtecki⊙,[d] Patrick Naulleau,[c]
and Slavomír Nemšák[b]

[a]University of California, Department of Physics, Davis, California, United States
[b]Lawrence Berkeley National Laboratory, Advanced Light Source, Berkeley,
California, United States
[c]Lawrence Berkeley National Laboratory, Center for X-Ray Optics, Berkeley,
California, United States
[d]International Business Machines—Almaden Research Center, San Jose,
California, United States

Abstract. The success in the miniaturization of the electronic device constituents depends mostly on the photolithographic techniques. Recently, to achieve patterning at the sub-10-nm node, extreme ultraviolet (EUV) lithography has been introduced into high volume production. Continued scaling of EUV via increased numerical aperture to achieve nodes at 3-nm and below requires the development of fundamentally new patterning materials and new characterization methods. Current EUV-resist film thicknesses are in the 20- to 40-nm range, and further thickness reduction is required for the next generation. Therefore, interfaces become exceedingly important, and the properties of the resist film would be dominated by top and bottom interfacial effects. X-ray photoelectron spectroscopy (XPS) combined with standing-wave excitation (SW-XPS), a fairly new method in the EUV lithography field, previously had been largely applied in multilayers and superlattices for characterizing the composition and electronic structure of buried layers and interfaces as a function of depth. We applied the SW-XPS method to organic/inorganic photoresists to provide depth-selective information on their structural and chemical conditions of as a function of temperature, EUV exposure, different underlayers, and other fundamental parameters. As a first attempt, we perform an SW-XPS feasibility study on self-assembled monolayer (SAM) films after exposure to an electron beam. By SW-XPS, we determined that the interface between the Al_2O_3 underlayer and the SAMs is smooth, with a mean roughness of about 0.2 nm. Moreover, we determined that the SAM chains are, on average, tilted by ∼30 deg off the sample normal. The SW-XPS results also suggest that the SAM is not a perfectly aligned and uniform monolayer, with some areas having thickness higher than a single monolayer. We demonstrated that SW-XPS can provide useful information on ultrathin materials with high potential for being used as a characterization method of organic/inorganic photoresists.

1 Introduction

As predicated by Moore's law, in the last 50 years, the semiconductor industry has driven the continuous decrease in the size of transistors to make faster, smaller, and more affordable

*Address all correspondence to Giuseppina Conti, grconti@lbl.gov

computer chips. Over the decades, this scaling has been driven by a continuous shrinking of the wavelength of light used in the photolithography process, and most recently extreme ultraviolet (EUV) lithography utilizing 13.5-nm light has been introduced into high volume manufacturing.[1] Although the first generation of EUV relies on conventional polymer photoresists, it is widely believed that the continued scaling of EUV by increasing the numerical aperture to achieve the 3-nm node and below will require the development of fundamentally new patterning materials or at least exquisite new control and understanding of the polymer type materials used in high volume manufacturing today. Moreover, no matter the photoresist technology, continued scaling in the lateral dimension has also led to a commensurate reduction in resist film thickness as a result of both aerial image depth of focus limits as well as pattern collapse issues.[2] Current generation EUV resists typically operate with film thicknesses in the 20- to 40-nm range, and further reduction will surely be required as we push EUV to the next generation. At such thicknesses, the interfaces become exceedingly important and in fact there may be no such thing as bulk material anymore with the resist film instead being dominated by top and bottom interface effects. It is evident that full characterization of future resist materials will require new methods enabling ultrahigh longitudinal resolution with chemical sensitivity as well as the ability to characterize buried interfaces. To address these needs, we proposed the use of standing-wave x-ray photoelectron spectroscopy (SW-XPS). SW-XPS is an advanced x-ray technique widely used to characterize quantum materials and emergent phenomena at the interfaces.[3] To demonstrate the power of this technique, we applied it to a promising new patterning material based on self-assembled monolayers (SAMs). The ultrathin nature of SAMs (<5 nm) allows them to serve as a perfect example of the depth precision and sensitivity of the SW-XPS technique. SAMs have been proposed as part of a new bottom-up patterning approach that could contribute to EUV lithography in several ways.[4,5] For example, it circumvents the pattern collapse issue that results when thick resists and small features create high aspect ratio nanostructures with mechanical properties that cannot survive the development step. SAMs have also been demonstrated as a viable tool for interface engineering; for example, SAMs have been used to combat interfacial acid loss. Moreover, SAMs can be tailored to deposit only on specific substrates. Combined with area-selective atomic layer deposition, such area selectivity could allow features to be deposited on top of existing patterns without extralithography steps, reducing overlay errors and allowing for a more flexible overlay budget in the entire process. This characteristic could also be used to circumvent etch selectivity issues arising from conventional ultrathin resist platforms.

A very critical issue in developing new SAM materials for EUV is the interaction between the SAM and its underlayer. For instance, it has been suggested[6] that the resist molecules near the interface are susceptible to activation by electrons originating in the substrate. Understanding the physical and chemical processes at the SAM/substrate interface is fundamental to better modeling their effects on imaging performance. SW-XPS can then reveal structural changes as a function of irradiation such as decomposition or oxidation of species, densification, polymerization, or crystallization with a few Angstrom depth resolution, as has been previously demonstrated on solid/liquid interfaces.[7,8] As a feasibility study, in this paper, we present a simplified SW-XPS study on SAM on Al_2O_3 underlayer after exposure to an electron beam. Specifically, we focus our attention on the characterization of the interface between the Al_2O_3 underlayer and the SAMs and on the determination of the sample coverage.

2 Experimental

2.1 Standing-Wave X-Ray Photoelectron Spectroscopy

XPS is a well-established method for the investigation of chemical states and electronic structures of a variety of materials. One of the advantages of this technique is its surface sensitivity due to the strong interaction of the excited electron with the studied material. As a consequence, the excited electrons cannot travel large distances in the sample without losing part of their energy. In general, for excitation x-ray energies in the range of 250 to 2000 eV, XPS probing depth varies from a few Angstroms up to several nanometers, depending also on the material
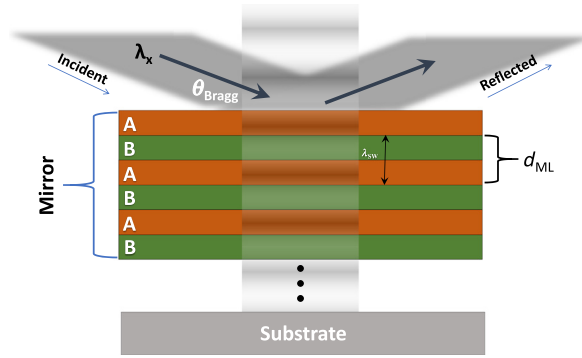
Fig. 1 Schematic of the Bragg-reflection standing-wave generator. The period of the multilayer mirror is connected to the wavelength and incident angle of x-rays via the Bragg condition. The period of the generated standing-wave is equal to the period of the multilayer structure.

under investigation. To enhance the depth-selectivity of measurements within the depth under consideration, the ideal method is the integration of the standing-wave technique with XPS. SW-XPS is based on spectroscopic analysis of photoelectrons excited by a strong standing-wave, which is generated by a Bragg-reflection off a synthetic multilayer mirror (Fig. 1).[9] The incidence angle and incident photon energy (wavelength) are related by the first-order Bragg condition:

$$\lambda_x = 2d_{\mathrm{ML}} \sin \theta_{\mathrm{inc}}, \tag{1}$$

where λ_x is the incident photon wavelength, d_{ML} is the period of the multilayer mirror, and θ_{inc} is the grazing incidence angle. In this way, the x-ray reflectivity is drastically enhanced and a strong standing-wave with vertically positioned nodes and antinodes is created along the multilayer mirror.

Once the standing-wave is generated along the multilayer mirror, it can be moved vertically through the sample by varying the incidence angle of the x-ray beam by half of the standing-wave period. As the antinodes of the electromagnetic field shift vertically through the sample, they highlight various parts of the sample, resulting in depth specificity of the photoemission signal. The period (or wavelength) of the standing-wave is equal to the period of the multilayer mirror, which allows us to engineer the period of the standing-wave suitable for each sample characterization. The vertical resolution of this depth-selective photoemission method approaches 1/10 of the standing-wave period, giving vertical resolution similar to transmission electron microscopy with the advantage of no sample preparation or modification.[10]

The dependence of the x-ray intensity (or electric field strength) as a function of incident angle and depth provides a unique intensity profile. The overall amplitude, width, and shape of these intensity profiles for specific species are determined by the optical properties of the sample, the position of the atoms in the layer, and the degree of interdiffusion of the sample with the upper (vacuum) or under layers (substrate). Quantitative structural and interface information can be determined from the experimental rocking curves (RCs) by matching them to simulated RCs using YXRO and Black Box Optimizer programs.[8,11]

2.2 *Sample Preparation*

[Si/Mo]$_{80}$ multilayer mirrors with a period of 3.4 nm were prepared by magnetron sputtering and used as standing-wave generators. The [Si/Mo]$_{80}$ multilayer mirror terminates with the Si layer on top, and the native SiO_2 was not removed. Multilayer mirrors were then coated with the Al_2O_3 layer of about 50 Å thickness deposited by atomic layer deposition at $T = 100°C$. Hydroxamic acid monolayer solutions were prepared at a concentration of 0.1 wt. %. in 4-methyl-2-pentanol. Al_2O_3-coated multilayer mirrors samples were immersed in a monolayer solution for a period of 18 h. After removing the samples from the solution, the samples were rinsed with isopropanol and dried under nitrogen. E-beam exposures were performed on a Raith e-beam direct write

lithography tool at a dose of 5000 mC/cm². The e-beam exposure was a blanket exposure over a 1×1 cm area. Based on previous data,[12,13] the same chemical behavior occurs during e-beam exposures as it does under EUV.

2.3 *XPS Measurements*

The SAMs were characterized at the synchrotron advanced light source (ALS) at Berkeley, California, using HAXPES endstation at the bending magnet beamline 9.3.1. We used p-polarized x-rays with photon energy of $h\nu = 3000$ eV. The inelastic mean free path of photoelectrons depends primarily on their kinetic energy and the density of the material, and in this case, it ranges from 30 to 68 Å, allowing us to reliably characterize the top SAMs film and its interface with the Al_2O_3 underlayer.[14] The total instrumental energy resolution was 600 meV. The exciting radiation was incident on the sample close to the Bragg peak at the grazing angle of 3.7 deg measured from the sample surface plane, and the photoemitted electrons were collected by a Scienta SES 2002 spectrometer along the sample normal. Being aware of the possible beam damage that can be caused by the x-ray excitation beam, we measured survey spectra before, during, and at the end of the experiment. We did not observe any variations in peak intensities or position between the first and last survey spectra, so we concluded that the low brightness beam of the bending magnet at beamline 9.3.1 at ALS did not damage the SAM sample.

3 Results and Discussion

The initial characterization of the SAM film on the substrate involved conventional core-level XPS measurements. Figure 2 shows the photoemission spectra of the core-levels originating from the multilayer substrate (Si 1s, Mo $3p_{1/2}$), from Al_2O_3 buffer layer (Al 1s, O 1s), and of the SAMs (C 1s, O 1s).

Spectral decomposition was done using Shirley background subtraction and fitting Voigt spectral shapes to the measured data. The peak fitting reveals two components in Si 1s spectra: the peak at low-binding energy is attributed to the elemental Si from the multilayer and that at high-binding energy is attributed to the oxidized Si from the topmost mirror layer. Two components in Mo $3p_{3/2}$ are due to two chemical states of molybdenum (Mo metal and $MoSi_x$ in the multilayer mirror). O 1s also exhibits two components: the peak at low-binding energy comes from the $Al_2O_3 + SiO_2$ under-layers and that at higher binding energy comes from the SAM and possible surface contaminants. The other core-levels (C 1s, Al 1s) show predominantly a single Voigt-like spectral shape. In principle, the C 1s spectrum of hydroxamic acid should present multiple spectroscopically distinctive species; however, to resolve these multiple chemical states, a dedicated higher resolution XPS study is needed.

Figure 3(a) shows the schematics of the SW-XPS experiment together with the sample configuration. The core-level regions (as shown in Fig. 2) were measured for each incidence angle, which is varied in SW-XPS experiments across the first-order Bragg peak. The integrated
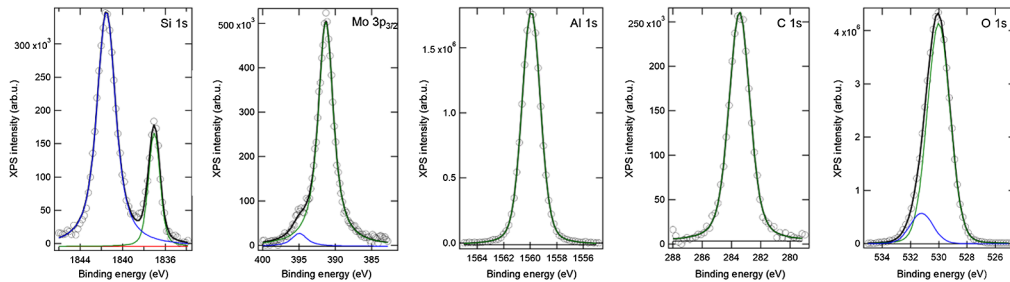

Fig. 2 XPS core level spectra of Si 1s, Mo 3p, Al 1s, O 1s, and C 1s measured at $h\nu = 3000$ eV after e-beam exposure of SAM film. Spectra shown after Shirley background subtraction; all peaks are fitted with Voigt spectral shapes.

intensity of the selected representative core levels was then plotted versus the incident angle, generating the RCs shown in Fig. 3(b). All of the RCs show a maximum or minimum at the incidence angle 3.7 deg that corresponds to the Bragg peak of the 3.4-nm $[Si/Mo]_{80}$ multilayer mirror. In addition, we observe that the RCs show different phases and modulations; for instance, the RCs of Al 1s and C 1s are very distinctive in phase, correctly indicating that they originate from adjacent but different depths in the sample. For a more comprehensive picture of the chemical and density profile, a full quantitative data analysis must be performed.

We used the YXRO software package[8] for x-ray optical and photoemission calculations. The structural model of the sample was based on the nominal thicknesses of the respective layers of the sample. The experimental and calculated RCs were then iteratively compared, and the structural parameters of the model (thickness of layers and roughness of interfaces) were optimized using a global black box optimizer.[10] The quality of the fit between the experimental and calculated RCs was measured by a conventional squared-deviation R-factor. Figure 3(b) shows the final results for the experimental RCs (circles) and calculated RCs (solid lines) calculated by YXRO based on the optimized model. The agreement between the experimental RCs and the simulations is very good. The final best-fit parameters of the structural model thus provide quantitative information on the constituent layers and on the interfaces, including mixing or roughness at the interfaces. The results from the optimized depth profile are reported in Fig. 3(c).

There are several interesting observations that can be concluded from this feasibility experiment. First, we confirmed indeed that the interface between Al_2O_3 and SAM film is sharp as expected with a mean roughness of only 0.2 nm. The mean thickness of the SAM was found to be around 1.8 nm. Based on the calculated chain length $-(CH_2)_n-$, in trans planar orientation we would expect a thickness of ~2.4 nm. Since the polymethylene part of the SAM's molecules is fairly rigid and the layer is well-compacted, the most likely explanation for this discrepancy is that molecules do not stand up perpendicular to the surface, but instead, on average, they are tilted by ~30 deg with respect to the sample normal.[15–18] Another interesting observation is that the SAM film has a much larger surface roughness (~1 nm), which means that molecules are not strictly assembled in a single-monolayer, but there are some deviations from this perfect ordering and self-limiting process such as some molecules forming a second layer. Last, a good agreement between experimental and calculated RCs for the core levels of the multilayer mirror confirms that our model successfully captures the chemical and structural parameters (thickness, intermixing, etc.) of the mirror, which is a critical prerequisite for the precise sub-nm depth analysis based on the SW-XPS technique.
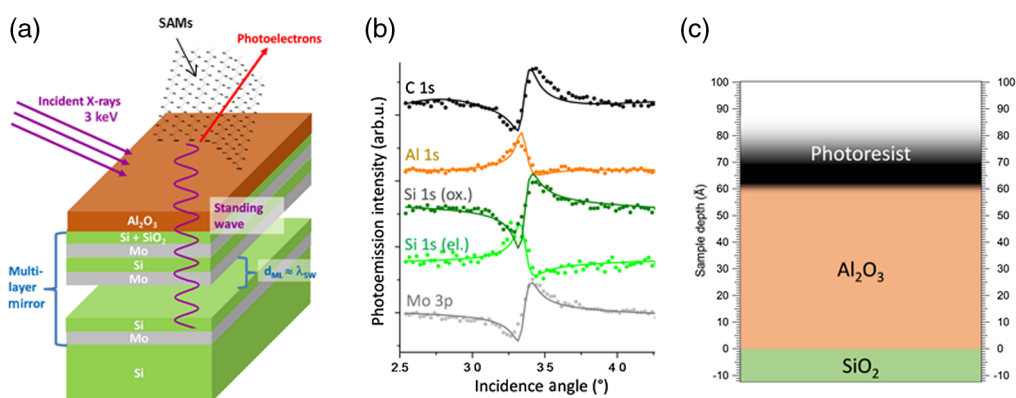

Fig. 3 (a) Schematic of the experimental configuration. The strong standing-wave perpendicular to sample surface is generated using first-order Bragg reflection with the period that equals the periodicity of the multilayer mirror. Nodes and antinodes of the standing-wave are swept vertically by changing the incident angle of x-rays. (b) Experimental (full circles) and simulated (solid lines) RCs of e-beam exposed SAM. (c) Concentration depth profile of top three layers: SAM, Al_2O_3 layer, and silica, showing their respective thicknesses and interdiffusion lengths (as color gradients).

4 Conclusions

SAM photoresist deposited on Al_2O_3 was used as a case-study example to demonstrate high-precision depth analysis based on SW-XPS. Measurements revealed, without any special sample preparation, that the interface between the Al_2O_3 underlayer and the SAMs is smooth as expected, with a mean roughness of only 0.2 nm. Moreover, we determined that molecules are, on average, most likely tilted at $\sim$30 deg off the sample normal. The results also suggest that the SAM is not a perfectly aligned and uniform monolayer, with some areas having a thickness higher than a single monolayer.

We demonstrated that x-ray standing-wave photoemission provides a nondestructive (in terms of sample preparation) way to probe chemical information with sub-nm depth resolution. It is a quantitative method, both in terms of absolute depth as well as absolute concentration. Due to its chemical and elemental sensitivity, this method is perfect for discovering chemical gradients, imperfections, and contaminants as well as roughness or interdiffusion at buried interfaces, helping the development of new organic/inorganic materials for EUV lithography application in the semiconductor industry.

References

1. E. A. De Silva et al., "Study of resist hardmask interaction through surface activation layers," *Proc. SPIE* **10809**, 1080916 (2018).
2. C. Wagner et al., "EUV lithography at chipmakers has started: performance validation of ASML's NXE:3100," *Proc. SPIE* **7969**, 79691F (2011).
3. C. S. Fadley and S. Nemšák, "Some future perspectives in soft-and hard-x-ray photoemission," *J. Electron Spectrosc. Relat. Phenom.* **195**, 409–422 (2014).
4. R. J. Wojtecki et al., "Additive lithography–organic monolayer patterning coupled with an area-selective deposition," *ACS Appl. Mater. Interfaces* **13**, 7, 9081 (2021).
5. R. J. Wojtecki et al., "EUV-patterning of monolayers for selective atomic layer depositing," Patent Pub. No.: US 2019/0391494 Al (2019).
6. J. Ma et al., "Engineering resist-substrate interface: a quantum chemistry study of self-assembled monolayers," *Proc. SPIE* **11517**, 115170H (2020).
7. S. Nemšák et al., "Concentration and chemical-state profiles at heterogeneous interfaces with sub-nm accuracy from standing-wave ambient-pressure photoemission," *Nat. Commun.* **5**, 5441 (2014).
8. G. Conti et al., "Sub-nm depth characterization of EUV nanoscale photoresist films by standing-wave photoemission spectroscopy," *Proc. SPIE* **11517**, 115170I (2020).
9. S.-H. Yang et al., "Making use of x-ray optical effects in photoelectron-, Auger electron-, and x-ray emission spectroscopies: Total reflection, standing-wave excitation, and resonant effects," *J. Appl. Phys.* **113**, 073513 (2013).
10. F. Kronast et al., "Depth-resolved soft x-ray photoelectron emission microscopy in nanostructures via standing-wave excited photoemission," *Appl. Phys. Lett.* **93**, 243116 (2008).
11. O. Karslıoğlu et al., "An efficient algorithm for automatic structure optimization in x-ray standing-wave experiments," *J. Electron Spectrosc. Relat. Phenom.* **230**, 10 (2019).
12. B. F. Porter, N. Mkhize, and H. Bhaskaran, "Nanoparticle assembly enabled by EHD-printed monolayers," *Microsyst. Nanoeng.* **3**, 17054 (2017).

13. R. J. Wojtecki, N. F. F. Nathel, and E. A. De Silva, "Polymerizable self-assembled monolayers for use in atomic layer deposition," Patent No: US 10,782,613 B2 (2020).
14. H. Shinotsuka et al., "Calculations of electron inelastic mean free paths. X. Data for 41 elemental solids over the 50 eV to 200 keV range with the relativistic full Penn algorithm," *Surf. Interf. Anal.* **47**, 871 (2015).
15. A. Ulman, "Formation and structure of self-assembled monolayers," *Chem. Rev.* **96**(4), 1533 (1996).
16. D. K. Schwartz, "Mechanisms and kinetics of self-assembled monolayer formation," *Annu. Rev. Phys. Chem.* **52**, 107 (2001).
17. S. G. J. Mathijssen et al., "Monolayer coverage and channel length set the mobility in self-assembled monolayer field-effect transistors," *Nat. Nanotechnol.* **4**, 674 (2009).
18. W. Senaratne, L. Andruzzi, and C. K. Ober, "Self-assembled monolayers and polymer brushes in biotechnology: current applications and future perspectives," *Biomacromolecules* **6**(5), 2427 (2005).